Quantitative DNA Methylation Analysis of *FOXP3* as a New Method for Counting Regulatory T Cells in Peripheral Blood and Solid Tissue

Georg Wieczorek,[1] Anne Asemissen,[2] Fabian Model,[11] Ivana Turbachova,[1] Stefan Floess,[3] Volker Liebenberg,[4] Udo Baron,[1] Diana Stauch,[2] Katja Kotsch,[2] Johann Pratschke,[5] Alf Hamann,[3] Christoph Loddenkemper,[7,8] Harald Stein,[7] Hans Dieter Volk,[2,6] Ulrich Hoffmüller,[1] Andreas Grützkau,[9] Alexander Mustea,[10] Jochen Huehn,[3] Carmen Scheibenbogen,[2] and Sven Olek[1,10]

[1]Epiontis GmbH; [2]Institut für Medizinische Immunologie and [3]Experimentelle Rheumatologie, Campus Mitte, Charité-Universitätsmedizin Berlin; [4]Epigenomics AG; [5]Department of Surgery and [6]Berlin-Brandenburg Center for Regenerative Therapies, Campus Virchow Klinikum, Charité-Universitätsmedizin Berlin; [7]Institut für Pathologie and [8]Research Centre ImmunoSciences, Campus Benjamin Franklin, Charité-Universitätsmedizin Berlin; [9]Deutsches Rheuma-Forschungszentrum; and [10]Tumorbank Ovarian Cancer, Berlin, Germany and [11]ocCure GmbH, Potsdam, Germany

Abstract

Regulatory T-cells (Treg) have been the focus of immunologic research due to their role in establishing tolerance for harmless antigens versus allowing immune responses against foes. Increased Treg frequencies measured by mRNA expression or protein synthesis of the Treg marker FOXP3 were found in various cancers, indicating that dysregulation of Treg levels contributes to tumor establishment. Furthermore, they constitute a key target of immunomodulatory therapies in cancer as well as transplantation settings. One core obstacle for understanding the role of Treg, thus far, is the inability of FOXP3 mRNA or protein detection methods to differentiate between Treg and activated T cells. These difficulties are aggravated by the technical demands of sample logistics and processing. Based on Treg-specific DNA demethylation within the *FOXP3* locus, we present a novel method for monitoring Treg in human peripheral blood and solid tissues. We found that Treg numbers are significantly increased in the peripheral blood of patients with interleukin 2–treated melanoma and in formalin-fixed tissue from patients with lung and colon carcinomas. Conversely, we show that immunosuppressive therapy including therapeutic antibodies leads to a significant reduction of Treg from the peripheral blood of transplantation patients. In addition, Treg numbers are predictively elevated in the peripheral blood of patients with various solid tumors. Although our data generally correspond to data obtained with gene expression and protein-based methods, the results are less fluctuating and more specific to Treg. The assay presented here measures Treg robustly in blood and solid tissues regardless of conservation levels, promising fast screening of Treg in various clinical settings. [Cancer Res 2009;69(2):599–608]

Introduction

Regulatory T cells (Treg) are an essential component of the immune system, balancing necessary aggressiveness against foes with tolerance for self-constituents (1). Pathologic imbalances of Treg are found in two major disease classes, i.e., autoimmune diseases and cancers. Whereas in autoimmune diseases, low Treg levels contribute to the failure to protect the body from its own defense mechanisms (2–4), recent studies indicate an overrepresentation of Treg in the peripheral blood of patients with solid tumors (5–10). Furthermore, an increased accumulation of Treg in the tumor mass goes along with an adverse prognosis (11, 12). Those observations not only contradict the concept of immunoignorance, but they suggest an alternative functional explanation for tumor immunity: tumor-induced dysregulation would exhibit tolerance, impeding a self-protective immune response. The tumor development thus would be promoted in part by the immune system itself, i.e., the suppressive function of Treg. Thus, Treg could be an important variable to be measured in diagnostic and patient monitoring settings.

An increasingly explored option for the therapy of solid tumors and other diseases is the modulation of the immune system. For instance, patients with melanomas and kidney cancer are treated by the administration of an immunostimulatory cytokine interleukin 2 (IL-2), which is thought to activate natural killer (NK) cells and T cells. Recent reports suggest that Treg proliferation is also triggered by IL-2, which would constitute an adverse effect for the intended immune activation of the therapy (13–16). A converse approach is pursued in immunosuppression therapies for transplantations, in which the intention is to abrogate host versus graft and graft versus host reactions. For that, T lymphocytes are blocked or eliminated. Modern therapies use antibodies, such as thymoglobuline (rabbit ATG) and basiliximab. rATG is a polyclonal antibody reactive against a variety of T-cell antigens and has been shown to efficiently eradicate T-lymphocytes (17). Basiliximab is a chimeric mouse human monoclonal antibody directed against the IL-2Rα (CD25; ref. 18). Binding of basiliximab to its target effectively inhibits T-cell signaling. In order to judge the efficacy of those therapies, it is important to measure the actual cellular effects of both stimulation (such as IL-2 treatment) and immunosuppression (basiliximab and rATG). Accordingly, immunomonitoring strategies are a crucial diagnostic and analytic component during the development or even in the clinical routine application of those therapies. Within the monitoring concepts, it is of particular value to quantitatively determine Treg because—in healthy individuals—they are naturally responsible for the regulation of an adequate immune response. However, precise Treg measurement has thus far remained awkward. Initially, $CD4^+$ Treg were characterized by high expression levels of CD25, which is a

Note: J. Huehn, C. Scheibenbogen, and S. Olek are senior authors.

Current address for S. Floess and J. Huehn: Helmholtz Centre for Infection Research, Experimental Immunology, Braunschweig, Germany.

Requests for reprints: Sven Olek, Epiontis GmbH, Rudower Chaussee 29, 12489 Berlin, Germany. Phone: 49-30-6392-3470; Fax: 49-30-6392-3476; E-mail: sven.olek@epiontis.com.

doi:10.1158/0008-5472.CAN-08-2361

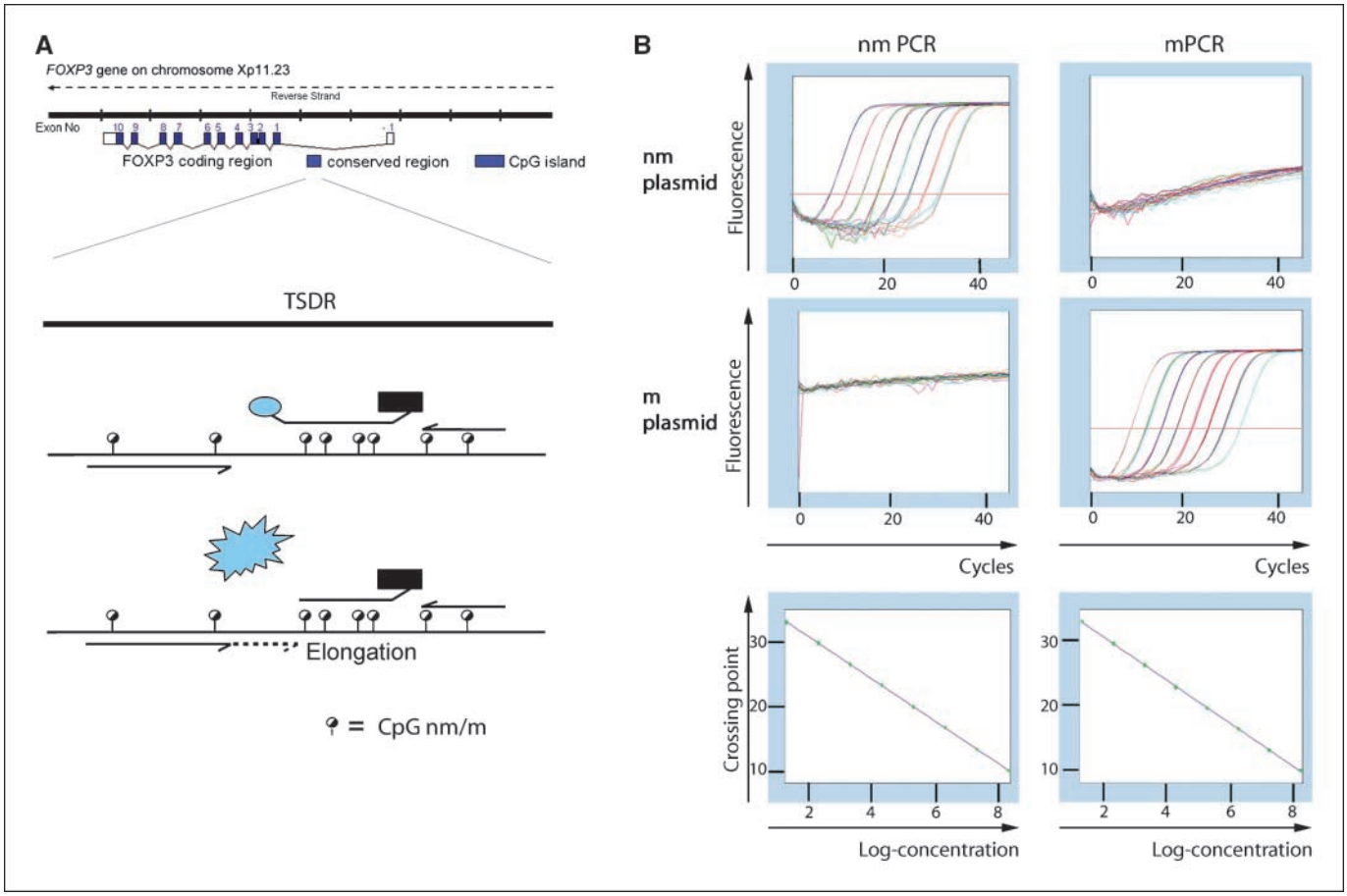

Figure 1. qPCR system for the *FOXP3* TSDR to detect Treg. *A,* schematic overview of the *FOXP3* locus and the amplification strategy. Two methyl-sensitive amplification primers and methyl-sensitive hybridization probes were designed. *Lollipops,* targeted CpG sites. The detection dye, which is quenched as long as the probe is intact, is released upon exonuclease digestion during specific strand elongation. *B,* amplification profiles of the qPCR systems (*top* and *middle*). *Left,* nonmethylation-specific amplification system; *right,* methylation-specific amplification system. *Top,* a plasmid corresponding to nonmethylated (*nm*) *FOXP3* TSDR DNA (all Cs in the TSDR are replaced by T) is used in a serial dilution row ranging from 200 million to 20 copies. *Middle,* the same dilution with a plasmid corresponding to methylated (*m*) *FOXP3* TSDR DNA (all Cs other than in the context of CG are replaced by T). *Bottom,* standard curves as produced by serial dilutions of plasmid present themselves in a strictly log-linear fashion.

component of the high-affinity IL-2 receptor (1). Although CD25 has always been known to be a rather unspecific activation marker, the identification of the forkhead box transcription factor (FOXP3)—as a constitutively expressed master switch for Treg development—has provided a powerful marker and an essential tool for analyzing and understanding the role of Treg (19–22). The specificity of FOXP3 expression in Treg was shown in the murine immune system using transgenic animals harboring *FOXP3* promoter–driven reporter genes (23). High levels of FOXP3 expression were also found in human natural $CD25^{high}CD4^{+}$ Treg. As a marker for human Treg, however, FOXP3 mRNA expression and protein synthesis is of doubtful value, due to the transient expression of FOXP3 in activated nonregulatory effector T cells (24–26). Thus, in the absence of a specific Treg marker, the interpretation of $FOXP3^{+}$ and/or $CD25^{+}$ Treg remained ambiguous because the measurements employed determine a mixture of activated conventional T cells and natural Treg. In addition, quantification of Treg by measuring FOXP3 and CD25 in solid tissues using immunohistochemical methods remains experimentally demanding, error-prone, and difficult to objectively standardize (27). Far-reaching clinical decisions within routine applications in such a setting are not in sight at present.

We have previously shown, both in mice and men, that stable expression of FOXP3 in naturally occurring Treg requires epigenetic, i.e., DNA methylation–based regulation (28, 29). DNA methylation is a biologically and chemically stable epigenetic modification, locking long-term gene expression patterns (30–32). Demethylation at a highly conserved region within the human *FOXP3* gene (Treg-specific demethylated region, TSDR; ref. 29) was found to be restricted to Treg when tested against all major peripheral blood cell types and a selection of non–blood cells. In addition to the high specificity for Treg, it was also observed that *FOXP3* TSDR demethylation occurred only in natural Treg, but not in recently activated effector T cells transiently expressing FOXP3 (28, 29). It was further associated with stable FOXP3 expression upon Treg expansion *in vitro*. These data indicated that epigenetic modifications in the *FOXP3* TSDR serve as a valuable marker for the identification of T cells with a stable Treg phenotype.

Here, we established a quantitative real-time PCR-based methylation assay, which enables the specific and sensitive determination of Treg numbers by measuring demethylated *FOXP3* TSDR DNA. We addressed the question of whether the methylation assay reliably reports Treg numbers in diagnostic or therapeutic settings, such as IL-2 therapy for patients with melanoma and

rATG or basiliximab treatment for transplantation patients. For the former, we used peripheral blood from patients with melanoma before and after completion of an IL-2 cytokine treatment. For the latter, we analyzed peripheral blood of patients prior to and after kidney or simultaneous kidney/pancreas transplantation, with the antibodies administered perisurgically. We further conducted a blinded study testing the notion that an increase of *FOXP3* TSDR demethylation in the peripheral blood would serve as an indicator for the establishment of malignancies in patients with manifested cancers compared with healthy controls. Finally, we conducted studies to evaluate this real-time PCR tool in its use to quantify the Treg number in formalin-fixed paraffin-embedded (FFPE) solid tissue samples, including both healthy and tumorous tissues.

Materials and Methods

Samples and Sample Preparation

Healthy donors. Peripheral blood samples were obtained from healthy donors after informed consent in accordance with local ethical committee approval. For the sorting of major peripheral blood leukocyte populations, samples were treated according to Baron and colleagues (29). Peripheral blood mononuclear cells (PBMC) were isolated by density gradient centrifugation using Ficoll-Hypaque (Sigma-Aldrich). $CD4^+$ T cells were isolated from PBMC by using anti-CD4 microbeads and the AutoMACS magnetic separation system (Miltenyi Biotec). All microbeads were purchased from Miltenyi Biotec and all antibodies for cell surface stainings were from BD PharMingen. Intracellular FOXP3 staining was performed with the PE anti-human FOXP3 staining set (eBioscience) and used according to the manufacturer's instructions. MACS-sorted $CD4^+$ T cells were stained using anti–$CD45RA^-$FITC and anti–$CD25^-$APC. Cells were sorted into $CD25^{high}CD45RA^-$ Treg and $CD25^-CD45RA^+$ naïve T cells by fluorescence-activated cell sorting (FACS; Aria, BD Bioscience). An aliquot of the CD4 population was used to determine the content of $FOXP3^+$ cells by flow cytometry; here, the analyzing gates resemble the sorting gates. Cytometric analysis was performed as previously described (33) using a FACSCalibur (BD Biosciences) and the FlowJo software (Tree Star).

For cell spiking, 10,000, 5,000, 2,500, 1,250, and 625 purified $CD25^{high}CD4^+$ cells were each mixed with 2 million isolated granulocytes corresponding to a Treg percentage of 0.5%, 0.25%, 0.13%, 0.06%, and 0.03%, respectively. Cell mixtures were subjected to genomic DNA isolation, followed by bisulfite treatment and methylation-sensitive *FOXP3* TSDR real-time PCR (see below). Template input per reaction corresponds to 56, 28, 14, 7, and (approximately) 3.5 copies of Treg DNA.

Patients with melanoma following IL-2 therapy. Patients with melanoma (five men and one woman; mean age, 52 years; ranging from 33 to 75) with stage IV metastatic disease, received IL-2 by s.c. administration with or without the addition of histamine dihydrochloride as described previously (34). After informed consent according to the local ethical guidelines, heparinized blood samples were drawn before and 2 weeks after the completion of a 4-week schedule of IL-2 therapy. PBMCs were isolated by density gradient centrifugation using Ficoll-Hypaque 1.077 (Biochrom or Sigma-Aldrich). For extracellular staining, the following surface monoclonal antibodies were used: anti–CD3-PercP (clone SK7), anti–CD25-PE (M-A251), and anti–CD4-FITC (B9.11). Nuclear anti–FOXP3-APC staining was performed according to the manufacturer's instructions using anti–FOXP3-APC (PCH101; eBioscience). Data acquisition was performed on FACSCalibur (BD Bioscience).

Transplantation patients under immunosuppressive therapy. Between October 2007 and May 2008, transplantation patients were recruited from the Department of Surgery and Nephrology, Virchow Klinik, Universitätsmedizin Charité, Berlin, and received a non-HLA identical allograft from a cadaveric donor. Transplant patients (three male patients; mean age, 48 $\pm$ 13) were first transplanted (kidney/pancreas) and received an initial 1.5 mg/kg body weight i.v. thymoglobulin (Genzyme) starting at day 0 followed by 4 further consecutive days. Patients for basiliximab therapies (n = 2 male, n = 4 female; mean age, 52 $\pm$ 11) were also first transplanted (kidney) and received two doses of basiliximab (20 mg i.v. 2 h before reperfusion and at day 4 posttransplantation). Maintenance immunosuppression in both groups consisted of tacrolimus, mycophenolate mofetil, and steroids. PBMCs were isolated by density gradient centrifugation using Ficoll-Hypaque 1.077 (Biochrom or Sigma-Aldrich). All experiments using human material were approved by the local ethical committee.

Peripheral blood analysis of cancer patients and healthy donors. Samples were obtained from the sources listed below and sample numbers received from each source are indicated in parentheses: Proteogenex (93), Universitätsklinik des Saarlandes (n = 1), Universitätsklinikum Schleswig-Holstein, Campus Lübeck (n = 2), Medizinische Hochschule Hannover (n = 18), and Universitätsklinikum Münster (n = 2). Written informed consent was obtained from all study participants adhering to the local ethical guidelines. Blood was collected in one or more 10 mL BD vacutainer tubes (BD Vacutainer Plus blood collection tube; Becton Dickinson) and each tube immediately inverted $\sim$10$\times$ to avoid blood clotting. The blood collection tubes were centrifuged at 1,500 $\times$ g for 10 min at 4°C with the centrifuge brake turned off. After centrifugation, $\sim$0.5 to 1 mL of fluid including the cellular layer between plasma and erythrocytes were transferred into a prelabeled 2 mL Cryo vial (Fisherbrand 2 mL round style bottom cryogenic storage vials; Fisher Scientific). Samples were frozen at −80°C within 4 h of the blood draw and stored at this temperature until shipped on dry ice. The sample collection consisted of 22 patients with breast cancer (22 women; mean age, 60; 18 patients with stage I to II disease and 4 patients with stage III or IV disease), 27 patients with colorectal cancer (13 men and 14 women; mean age 64; 13 patients with stage I or II and 14 patients with stage III or IV disease), 24 lung cancer patients (11 male and 13 females; mean age, 62; 9 patients suffering from stage I and II, 9 patients with stage III or IV, and 6 patients with no disease stage information), 23 prostate cancer patients (23 male; mean age, 65; 9 with stage I/II disease, 1 with stage III/IV disease, and 13 without stage information) and 20 normal controls (11 male and 9 female; mean age, 55).

FFPE tissues. FFPE samples from 15 patients with primary colorectal cancer and 5 patients with stages II to IV primary lung cancer were retrieved from the Pathology Department of Charité, Campus B.F., Berlin. Colorectal cancer tissues had been already analyzed in a previous study for FOXP3 expression using immunohistochemistry (35). FFPE control samples were either from adjacent healthy colon (five samples) and lung (one sample) tissue from the tested patients or healthy tissue from other colon (five samples) and lung (two samples) patients obtained during surgery. All patients with colorectal cancer (mean age, 55 years; range, 36–73) and controls (mean age, 58 years; rang, 48–76) were female. All lung controls (n = 3) were male (ages 61, 65, and 67), one lung cancer patient was female and four were male (mean age, 63 years; range, 52–74). For DNA isolation from FFPE tissues, up to eight tissue slices were used. Slices were incubated overnight in 50 mmol/L of Tris/HCl (pH 8), 1 mmol/L EDTA, 0.5% Tween 20 containing 2 mg/mL of proteinase K with subsequent incubation at 90°C for 10 min and DNA was purified with Qia-AMP DNA FFPE tissue kit (Qiagen) according to the manufacturer's protocol.

DNA Preparation from Blood and Bisulfite Conversion

Genomic DNA was isolated using the DNeasy blood and tissue kit (Qiagen). For PBMC and sorted blood cells, the protocol for cultured cells was followed. For DNA isolation from buffy coats, the whole blood protocol was used. Bisulfite treatment of genomic DNA was performed according to Olek and colleagues (36) with minor modifications.

Real-time PCR

Real-time PCR was performed in a final reaction volume of 20 μL using Roche LightCycler 480 Probes Master (Roche Diagnostics) containing 15 pmol each of methylation or non–methylation-specific forward and reverse primers for TSDR, 5 pmol of hydrolysis probe, 200 ng of lambda-DNA (New England Biolabs), and 30 ng of bisulfite-treated genomic DNA template or a respective amount of plasmid standard. Each sample was analyzed in triplicate using a LightCycler 480 System (Roche). Cycling

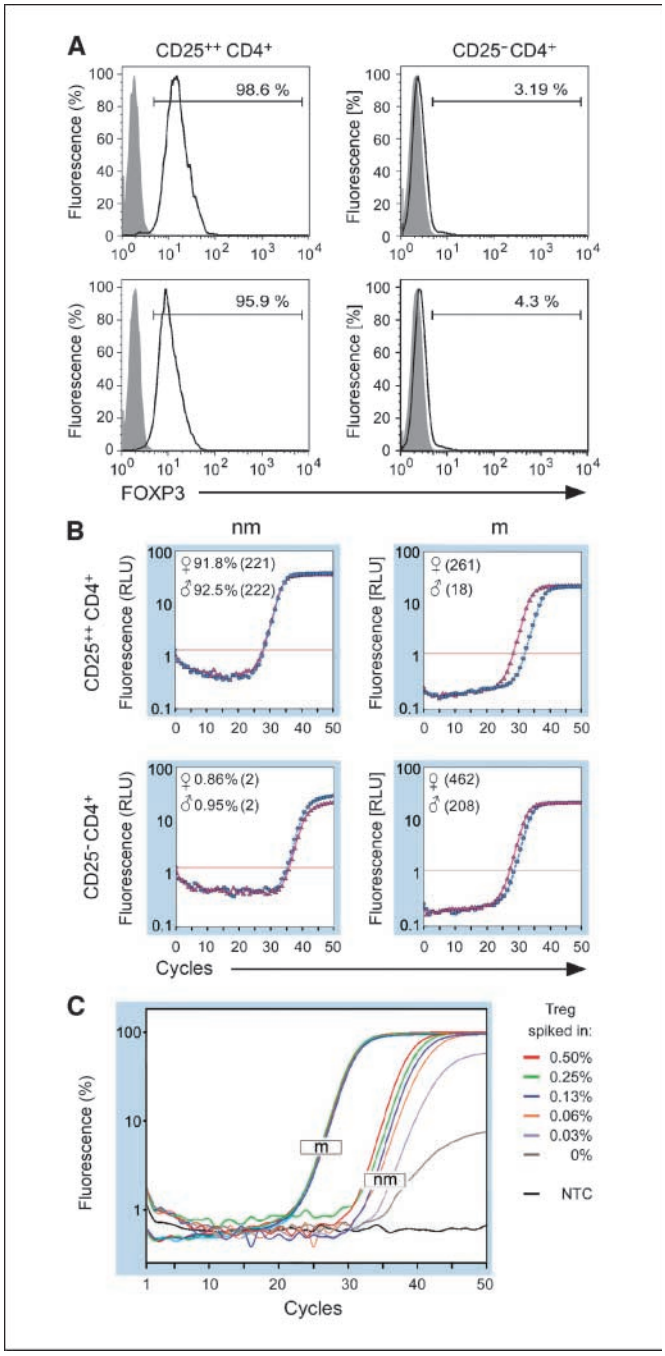

Figure 2. Treg determined by FACS and *FOXP3* TSDR demethylation. *A,* FACS analysis of $CD25^{++}$ (*left*) and $CD25^{-}$ (*right*) $CD4^{+}$ T cells from a male (*top*) and a female donor (*bottom*) after separation from PBMC (see Materials and Methods). Sorted cells were fixed and stained for intracellular FOXP3 expression. Numbers in the histograms indicate the percentage of $FOXP3^{+}$ cells. *B,* qPCR amplification plots for sorted $CD25^{++}$ cells and $CD25^{-}CD4^{+}$ T cells, each for the male (*blue line*) and female (*red line*) donor presented in *A*. Numbers in the plots indicate the calculated percentages of Treg as determined by qPCR (see Materials and Methods). Numbers in parentheses represent the measured copy numbers for nonmethylated DNA (*nm; left*) and methylated DNA (*m; right*). *C,* spiking experiment to explore the limit of Treg detection: 200,000 granulocytes (methylated *FOXP3* TSDR) were added to gradually decreasing numbers of Treg (demethylated *FOXP3* TSDR) and were subjected to qPCR analysis. *Right,* color code indicates the percentage of Treg added (for details, see Materials and Methods). *NTC,* control without template DNA. Amplification profiles for unmethylated template DNA (*nm*) show a linear right shift along the *X*-axis reflecting the gradual decrease of Treg added. For methylated template DNA (*m*), amplification curves overlap at an identical cycle number for all cell mixtures.

conditions consisted of a 95°C preheating step for 10 min and 50 cycles of 95°C for 15 s followed by 1 min at 61°C. Methylation-specific and demethylation-specific amplification primers for TSDR map to the following chromosomal positions: NCBI36:X:49004163-49004190:1 (forward primers) and NCBI36:X:49004227-49004251:1 (reverse primers). Hydrolysis probes map to chromosomal position NCBI36:X:49004200-49004222:1 (demethylation-specific probe) and NCBI36:X:49004200-49004217:1 (methylation-specific probe).

Plasmid Standard

PCR products were generated with methyl– and non-methyl–specific primers for *FOXP3* TSDR using genomic, bisulfite-treated DNA from sorted naïve and regulatory T cells. DNA fragments were cloned into pCR2.1-TOPO vector, using TOPO TA cloning kit (Invitrogen) according to the manufacturer's instructions and verified by sequencing. Plasmids were purified with Qiagen Plasmid Midi Kit, the concentration was determined by Qubit fluorometer (Invitrogen) and diluted to obtain final concentrations of 100, 10, 1, and 0.1 fg representing 20,000, 2,000, 200, and 20 plasmid copies as standard for quantitative PCR (qPCR) reactions, each for methylated and nonmethylated *FOXP3* qPCR assay.

Statistical Analysis

Amounts of methylated and unmethylated *FOXP3* DNA were estimated from calibration curves by linear regression on crossing points from the second-derivative maximum method (37). The median was used to aggregate triplicate measurements of the buffy coat samples. The proportion of unmethylated DNA was computed as the ratio of unmethylated *FOXP3* TSDR-DNA and the sum of methylated and unmethylated *FOXP3* TSDR-DNA. For female patients, this ratio was corrected with a factor of 2 due to the fact that one of the two TSDR alleles is methylated as a result of X-inactivation.

For the quantitation of the *FOXP3* methylation-based discrimination between peripheral blood of cancer patients and normal controls, the area under the receiver operating characteristics (ROC) curve (AUC) value was used. Here, it is equivalent to the probability that a randomly selected cancer patient shows higher *FOXP3* methylation in peripheral blood than a randomly selected normal control. No discriminative ability corresponds to an AUC of 0.5. A perfect discrimination has an AUC of 1.0. AUCs were estimated by means of the trapezoidal rule. The Wilcoxon-rank sum test was used to compare demethylation rates between normal and cancer patients. The Wilcoxon signed-rank test was used to compare demethylation rates pre– and post–IL-2 treatment. For correlation analysis, Pearson's product moment coefficient and t test statistics were used. All P values are two-sided.

Immunohistochemistry

Immunohistochemical staining was performed as previously described (35). In brief, slides were incubated with the rat monoclonal antibody against human FOXP3 protein (PCH101, 1:200; eBioscience), followed by biotin-conjugated rabbit anti-rat and the EnVision peroxidase kit (Dako). Ten randomly selected high-power fields (1 HPF = 0.237 mm^2) were analyzed for $FOXP3^{+}$ cell infiltration in tumor tissue and matched normal colonic mucosa/lung parenchyma, and 10 HPF were averaged in each case.

Results

Methylation-sensitive *FOXP3* TSDR real-time PCR system. In order to quantitatively analyze the specificity of *FOXP3* TSDR demethylation to Treg, we established a real-time PCR system (qPCR). This system consists of methylation-dependent amplification primers and hybridization probes for both bisulfite-converted methylated and unmethylated DNA of the *FOXP3* TSDR (Fig. 1*A*). We tested this system on plasmids cloned from bisulfite-converted Treg and naïve T cell DNA. These clones contain sequences corresponding to unmethylated or methylated bisulfite-converted *FOXP3* TSDR. We showed high specificity, linearity

of amplification over six orders of magnitude, and no cross-reactivity with the opposite template species, even at unphysiologically high concentrations (ranging from 20 to 200 million copies of plasmid DNA; Fig. 1*B*).

With technical variables specified, we compared the performance of conventional FACS analysis for Treg detection with the *FOXP3* TSDR demethylation assay. For this, we used sorted $CD25^{high}CD4^+$ T cells and $CD25^-CD4^+$ conventional T cells from healthy male and female donors. Flow cytometry analysis revealed FOXP3 expression in >95% of $CD25^{high}$ Treg and up to 4.3% in $CD25^-CD4^+$ conventional T cells (Fig. 2*A*). Demethylation analysis confirmed these findings with ~93% of the $CD25^{high}$ Treg showing an unmethylated *FOXP3* TSDR in male donors and 45.9% in female donors (~92% of the cells, when corrected with a factor of 2 owing to inactivation and methylation of one X-chromosome). Among $CD4^+CD25^-$ cells, <1% were demethylated in the *FOXP3* TSDR (Fig. 2*B*). Treg content in $CD4^+CD25^{high}$ as determined by TSDR analysis is somewhat lower than observed with FOXP3 expression analysis, suggesting superimposition by activated non–Treg in the latter procedure. Equally, TSDR demethylation is lower in naïve T cells than determined by FACS analysis, suggesting that impurities retained during $CD25^-$ sorting mainly originated from $CD25^{medium}$ cells, which may express FOXP3 to some extent but are not exhibiting bona fide natural Treg with the $CD25^{high}$, *FOXP3* TSDR demethylated Treg phenotype. However, altogether, a good correlation between both detection methods was observed.

Next, the assay sensitivity was tested in an *in vitro* system. For this, we added a gradually decreasing amount of sorted Tregs into a constant number of control cells (granulocytes), which have been shown to be completely methylated in the *FOXP3* TSDR (ref. 29; see also next paragraph). We robustly detected 0.5%, 0.25%, 0.13%, and 0.06% Treg. The detection limit was at 0.03% Treg corresponding to approximately 3.5 copies of unmethylated template DNA in 12,000 copies of methylated background DNA (Fig. 2*C*).

***FOXP3* TSDR demethylation in sorted blood cell subtypes.** For the presented assay, it is a prerequisite for Treg measurement in full blood that all non-Treg blood fractions are overwhelmingly methylated in the *FOXP3* TSDR. Thus, to characterize biological specificity, we analyzed the methylation level in various leukocyte fractions. Results are summarized in Table 1. Isolated $CD14^+$ monocytes, $CD15^+$ granulocytes, $CD56^+$ NK cells, and both $CD8^+$ memory ($CD27^+CD45RA^+$) and $CD8^+$ naïve ($CD27^+CD45RA^-$) cytotoxic T cell fractions showed <0.5% TSDR demethylation. $CD19^+$ memory and naïve B cell fractions comprise <2% demethylated TSDR. $CD4^+CD27^+CD45RA^+$ naïve T cells and $CD4^+CD27^+CD45RA^-$ memory T cells contain a demethylated fraction of 6.2% and 10.86%, respectively. Both fractions have previously been described to contain approximately 10% of $CD25^{high}$ $FOXP3^+$ Treg. Therefore, our measurements meet the expected rate of Treg in those fractions. As shown above in Fig. 2*B*, the selective removal of $CD25^{high}$ cells from the total $CD4^+$ cell fraction leads to the depletion of all cells with a demethylated *FOXP3* TSDR. This fact once more suggests the specificity of TSDR demethylation to $CD25^{++}$ cells. Taken together, it seems that only Treg are demethylated at the TSDR and a specific Treg measurement based on the TSDR demethylation should be feasible.

Table 1. *FOXP3* TSDR demethylation levels in major leukocyte cell types as determined by qPCR

Blood cell types	qPCR result (% demethylated *FOXP3* TSDR)
$CD4^+CD27^+CD45RA^+$ naïve T cells	6.2
$CD4^+CD27^+CD45RA^-$ memory T cells	10.86
$CD8^+CD27^+CD45RA^+$ naïve cytotoxic T cells	0.49
$CD8^+CD27^+CD45RA^-$ memory cytotoxic T cells	0.34
$CD15^+$ granulocytes	0.01
$CD14^+$ monocytes	0.06
$CD56^+$ NK cells	0.07
$CD19^+$ naïve B cells	1.96
$CD19^+$ memory B cells	1.34

***FOXP3* TSDR demethylation in patients with melanoma treated with IL-2.** Next, we studied the effect of IL-2 therapy on the frequency of $CD4^+CD25^{high}$ $Foxp3^+$ Treg in the PBMCs of six patients with metastatic melanoma using both FACS and TSDR demethylation analyses (Fig. 3*A*). Prior to therapy, FACS measurements of PBMC showed an average frequency of $CD4^+CD25^{high}$ $FOXP3^+$ cells of 4.5% (range, 1.9–8.9%; SD, 2.4%). After 4 weeks of an IL-2 therapy schedule followed by 2 weeks of reconvalescence, the levels of $FOXP3^+$ cells were measured again. Compared with pretherapy levels, FACS data showed a significant increase with an average of 11.6% of FOXP3 expressing cells (range, 5.1–17.3%; SD, 4.6%; $P = 0.03$). When Treg frequency was determined using the *FOXP3* TSDR demethylation assay in the same samples, the average demethylation ratio prior to IL-2 therapy was at 3.4% (range, 2.4–4.2%; SD, 0.7%). After IL-2 therapy, Treg levels were significantly increased showing an average demethylation level of 8.8% (range, 6.9–11.5%; SD 1.6%; $P = 0.03$). From two of these patients, $CD4^+CD25^{high}$ Treg were isolated by magnetic beads (MACS) before and after IL-2 therapy. In both patients, $CD4^+CD25^{high}$ cells showed similar demethylation values (from 87.5% to 88.3% and from 85.2% to 93.9%; data not shown). Taken together, cell numbers as measured by FACS and *FOXP3* TSDR demethylation correlate well (Pearson correlation $R = 0.65$, $P = 0.023$) and they seem to detect largely congruent cell populations (i.e., Treg). The previously reported increase of Treg upon IL-2 therapy was confirmed by two independent technological approaches.

***FOXP3* TSDR demethylation in immunosuppressed, solid organ–transplanted patients.** We counted Treg levels in transplantation patients treated with the immunomodulatory therapeutic antibodies thymoglobulin (rATG; three patients) and basiliximab (six patients) applying the *FOXP3* TSDR demethylation assay (Fig. 3*B*). When demethylation prior to and after ATG treatment was analyzed, we found that Treg levels decreased in all three patients. Pretherapy levels ranged from 0.6% to 7.6% and dropped to values <0.25% in each case. Statistical significance could not be reached due to the low number of patients ($n = 3$) included. When demethylation prior to and after basiliximab therapy was analyzed, we found a significant decrease of Treg levels ($P = 0.03$) for all samples with an average pretherapy demethylation level of ~1.6% (range, 0.6–4.3%), and an average posttherapy demethylation level of 0.66% (range, 0.02–2.2%). Taken together, we see a significant decline of Treg levels upon the described immunosuppressive therapies.

***FOXP3* TSDR demethylation in peripheral blood of patients with cancer and healthy donors.** Next, we tested if an up-regulation of Treg numbers was observed in the peripheral blood of patients suffering from solid tumors using the *FOXP3* TSDR demethylation assay. For this, we measured the methylation status of the *FOXP3* TSDR in the leukocyte fraction of a total of 115 blood samples from healthy controls, colorectal, lung, prostate, and breast cancer patients in a blinded study (for sample preparation and characteristics, see Materials and Methods). For healthy donors, the average Treg frequency was at 1.4%, ranging from 0.4% to 2.9%. For patients with colorectal cancer, the Treg concentration was at 2.3%, ranging from 0.6% to 3.5% with one outlier at 19%. Excluding the outlier, the average Treg frequency was at 1.6%, only slightly higher than for healthy donors. Treg concentration in lung cancer patients ranged from 0.5% to 4.4% with an average of 2.3%. Although results for patients with colorectal cancer did not significantly differ from normal controls, Treg frequencies in patients with lung cancer were significantly elevated ($P = 0.003$). ROC curves for colon and lung cancer show an AUC (see Materials and Methods: Statistical Analysis) of 0.66 for colon and an AUC of 0.75 for lung cancer (Fig. 4*A*). A separate analysis of Treg levels in male and female lung cancer patients and comparison with gender-matched controls shows similar AUC values (male lung cancer AUC = 0.73; female lung cancer AUC = 0.74); however, comparisons are no longer significant (male lung cancer $P = 0.076$; female lung cancer $P = 0.071$). When comparing Treg frequencies in breast and prostate cancer patients to healthy controls of the same sex, the average Treg concentration was elevated to 2.4% for both cancer types, compared with 1.7% in female and 1.4% in male normal controls. The changes, compared with normal individuals, were statistically significant for prostate cancer ($P = 0.03$) and slightly below significance for breast cancer ($P = 0.08$). ROC curves showed an AUC of 0.71 for discriminating between normal females and those with breast cancer and an AUC of 0.73 for discriminating between normal males and those with prostate cancer (Fig. 4*B*).

***FOXP3* TSDR demethylation in FFPE tissue samples.** Finally, we asked if measurement of *FOXP3* TSDR demethylation might resolve the technical issues encountered with current methods to detect Treg in solid tissues. We selected FFPE samples from non–small cell lung and colon carcinoma and corresponding adjacent normal tissue. On the one hand, samples were measured using immunohistochemistry, detecting the number of FOXP3$^+$ cells in tissue sections per HPF (Fig. 5*A*). On the other hand, we used material from the same paraffin blocks for Treg quantification by measurement of *FOXP3* TSDR demethylation. When using immunohistochemistry, higher concentrations of Treg were found in colorectal cancer tissue (average immunohistochemistry cell number, 15.3 Treg/HPF; range, 4.4–52 Treg/HPF) when compared with normal adjacent colon tissue (average immunohistochemistry cell number, 0.3 Treg/HPF; range, 0.1–0.6 Treg/HPF). When the concentration of Treg in colorectal cancer tissue was analyzed using *FOXP3* TSDR demethylation assay, an average demethylation of 6.3% was observed, ranging from 1.9% to 12.3%. In healthy control tissue, on average, 1.5% Treg were measured ranging from 0.8% to 2.8%. For both technologies, the tumor-specific increase of Treg infiltration is statistically highly significant ($P < 0.001$). For lung tissue, immunohistochemistry measurements showed an increase of Treg in tumor tissue (average immunohistochemistry cell number, 6.8 Treg/HPF; range, 3.9–10.1 Treg/HPF) compared with normal lung tissue (average immunohistochemistry cell number, 0.2 Treg/HPF; range, 0.1–0.4 Treg/HPF). Measured by *FOXP3* TSDR demethylation analysis, average Treg levels were at 3.8%, ranging from 1.6% to 6.4% for cancerous tissue and average demethylation levels were at 0.7% for healthy tissue, ranging from 0.5% to 0.8%. Despite the limited amount of lung tissue samples included in this study, the observed changes are statistically significant ($P = 0.036$ for immunohistochemistry and *FOXP3* TSDR demethylation). Further statistical analysis showed that the determination of FOXP3$^+$ cells by immunohistochemistry and *FOXP3* TSDR demethylation analyses are highly correlated (Pearson correlation $R = 0.80$; $P < 0.001$; Fig. 5*B*). To compare the performances of the technologies, we used the nonparametric test of DeLong (38). Immunohistochemical analysis showed a perfect separation between normal and cancerous tissues (AUC = 1.0). *FOXP3* TSDR methylation analysis showed an almost perfect separation (AUC = 0.96). Based on these two AUC values, there is no significant difference between the immunohistochemical and the *FOXP3* TSDR demethylation methods when analyzing normal

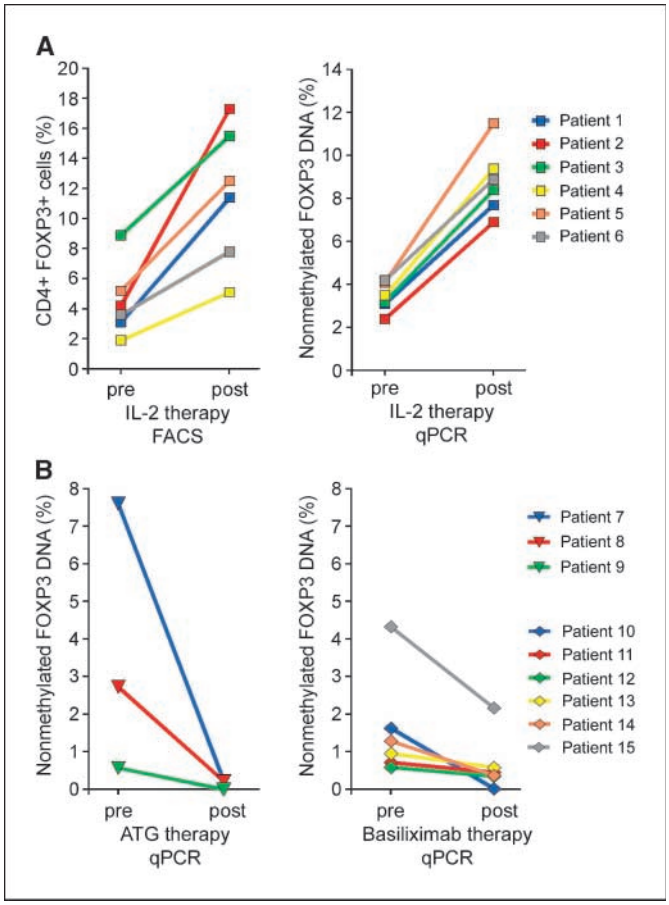

Figure 3. Treg in the peripheral blood of patients treated with immunomodulators. *A,* FOXP3$^+$ Treg frequencies measured on six patients with melanoma prior to and 2 weeks after completion of IL-2 therapy. *Left,* results from measurements by flow cytometry (*FACS*); *right,* Treg frequencies as measured by *FOXP3* TSDR qPCR. Both types of analyses were conducted on the same patient samples at identical time points. *B,* Treg frequencies of nine transplantation patients were quantified by *FOXP3* TSDR qPCR prior to and after a single treatment with thymoglobulin (*rATG; left*) or basiliximab (*right*), respectively. Posttherapy measurements were conducted 14 d (patient no. 7) and 11 d (patient nos. 8 and 9) after ATG medication. For basiliximab, posttherapy measurements were conducted 1 day post-medication except for patient no. 11, who was analyzed after 2 d.

control versus cancer tissue distinction (P = 0.17). Thus, the tissue data show that both measurement methods are equivalent as far as distinction is concerned.

Discussion

Over the last decade, Tregs have become a central focus of immunologic research and an important player in tumor immunity (1, 2, 15). In order to understand the role of Treg in disease settings, it is of paramount importance to be able to specifically detect and quantify the number of Tregs present in peripheral blood or disease-inflicted tissue. Once possible, Treg counts might serve as an important diagnostic and prognostic variable. However, current detection methods for Treg do not allow for exact quantification due to the absence of cell type specificity in the FOXP3 and CD25 mRNA and protein markers used (26, 27). All evidence from our previous studies (28, 29) suggested that demethylation of the *FOXP3* TSDR is exclusive for stable bona fide Treg. Thus, its measurement seemed highly suitable for the establishment of a quantitative Treg assay. When transformed onto a qPCR platform (Fig. 1), *FOXP3* TSDR demethylation showed high biological specificity to Treg when all major leukocyte fractions were analyzed. Residual *FOXP3* TSDR demethylation in cell types other than Treg, including B cells, is most likely attributed to incomplete purification by the flow cytometric sorting schemes used (Table 1). Physiologic Treg levels are assumed to range between 0.5% and 5% in the peripheral blood and at ~0.1% in healthy other tissues (27, 39, 40). Thus, the observed detection limit of the *FOXP3* TSDR demethylation assay (0.03%) qualifies for accurate Treg measurements in all clinical settings (Fig. 2). Although our analyses prove specificity within the blood components, eventually, it will be necessary to analyze the epigenetic profile of further, non-hematopoietic cell types to show the universal applicability of this system. This is particularly significant because recent data indicate that FOXP3 mRNA expression has been observed to act as a tumor suppressor in non-Treg in solid tissues (41), a fact that might or might not be reflected in the epigenetic pattern. The universal applicability of this assay might also be impaired by differences between male and female donors. The straight correction by a factor of 2, which we used to compensate for the X-inactivation, does not take into account possible biological differences between the two sexes, such as increased tolerance of foreign antigens during pregnancy, which might require elevated Treg levels (42). In awareness of the specifications and limitations referred to, we intended to use the newly developed assay in a number of possible routine applications in clinical settings.

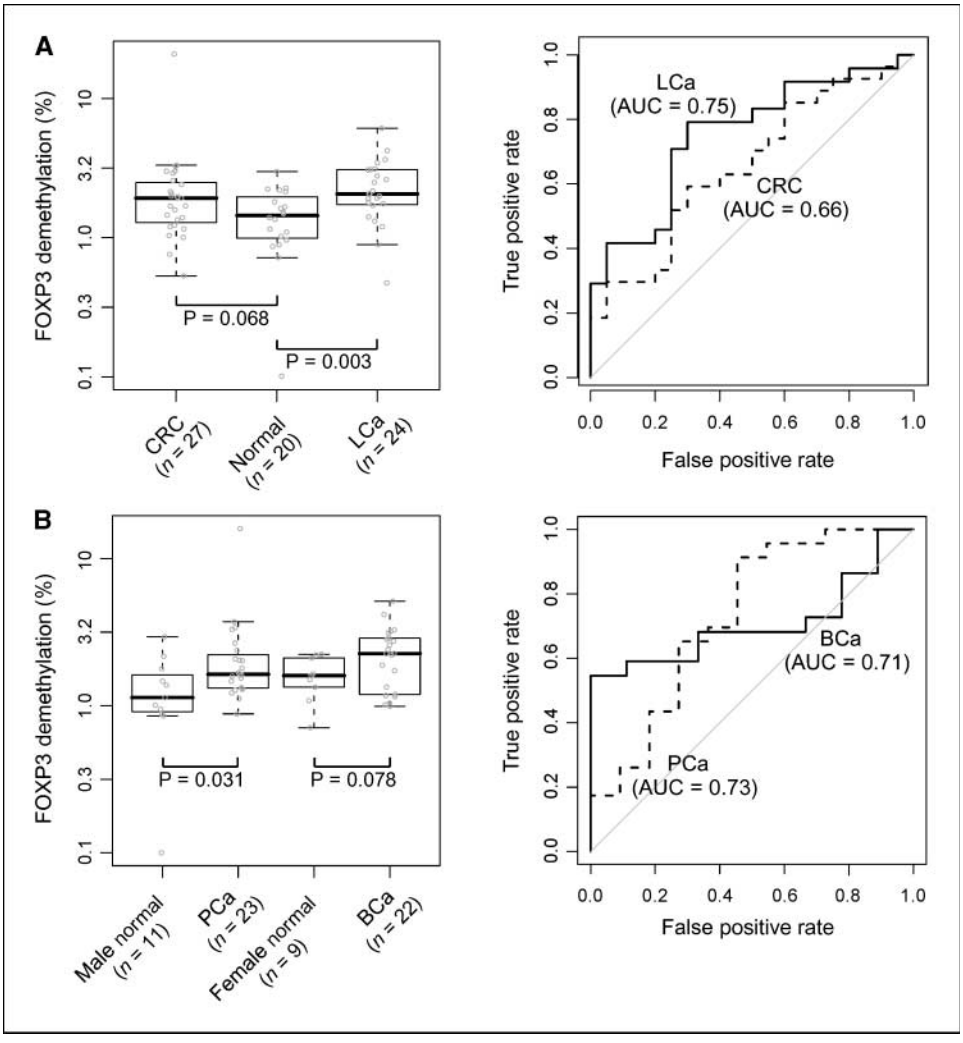

Figure 4. Treg in peripheral blood of healthy donors and patients with solid tumors. Treg levels were measured in the peripheral blood using the *FOXP3* TSDR demethylation assay (for exact sample preparation and sample characteristics, see Materials and Methods). *A, left,* box plots visualize the distribution of *FOXP3* TSDR demethylation levels grouped by patient diagnosis (normal controls; *CRC,* colorectal cancer; *LCa,* lung cancer; patient numbers for the respective groups in parentheses). *Vertical axis,* percentage of demethylation. *Individual box plots,* middle 50% of the data; *middle line,* median. Whiskers extend to the most extreme data point which is no more than 1.5 times the interquartile range from the box. *Gray points,* individual measurement values. *P* values indicating statistical significance for group discrimination (*box plots*). *Right,* ROC curves are plotted for the discriminations between normal controls and cancer patients. AUC values reflecting group discrimination are indicated. *B,* the box plots visualize the distribution of *FOXP3* demethylation levels grouped by patient diagnosis (*PCa,* prostate cancer; *BCa,* breast cancer) and the respective normal, gender-matched controls. Patient numbers for the respective groups are indicated in parentheses. Normal controls in *A* and *B* are identical. *P* values indicating statistical significance for group discrimination (*box plots*). *Right*, the ROC curves are plotted for the discriminations between female normal controls and patients with breast cancer and for the discriminations between male normal controls and patients with prostate cancer. AUC values reflecting group discrimination are indicated.

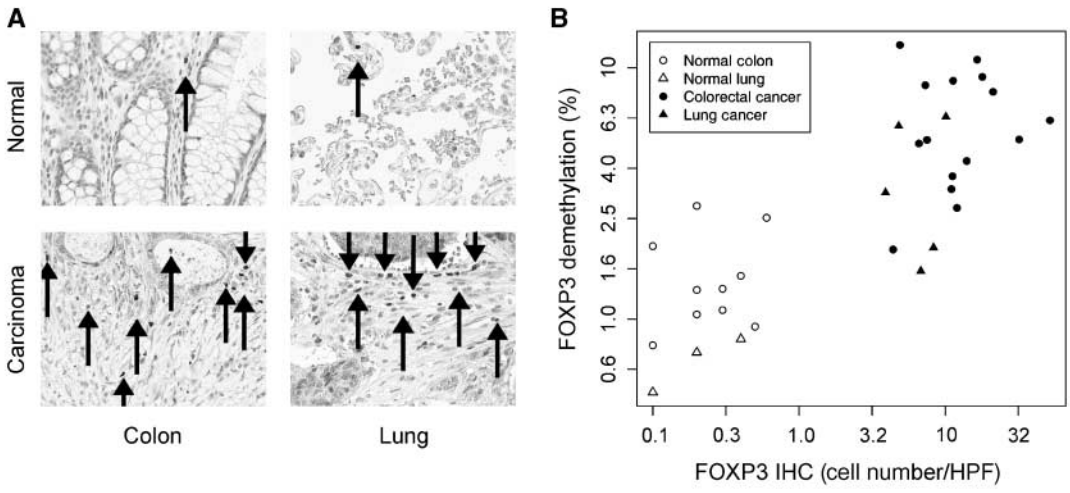

Figure 5. Treg in FFPE tissue samples. *A,* representative immunohistochemically stained tissue sections. Only a single FOXP3-stained cell is seen in each healthy colon (*top left*) and lung (*top right*) tissue. *Arrows,* single FOXP3-stained cells. In cancerous colon and lung tissues (*bottom left* and *bottom right*, respectively), FOXP3$^+$ cells are more abundant (*arrows,* selected FOXP3$^+$ cells). *B,* correlation between Treg concentrations measured by FOXP3 immunohistochemistry (*IHC*) and DNA methylation analysis for the set of normal adjacent colon tissue samples (○), normal lung tissue samples (△), colorectal cancer tissue samples (●), and lung cancer tissue samples (▲). *Horizontal axis,* average number of Treg cells per HPF, determined by averaging FOXP3 antibody–stained cell numbers over 10 HPFs. *Vertical axis,* the *FOXP3* TSDR demethylation rate in the respective sample.

We measured blood samples from melanoma patients that had received IL-2 treatment. Although aiming at enhancing NK and T cell responses, recent observations suggested a significant increase of Treg numbers following IL-2 treatment (13, 16). These observations ignited a debate as to whether this treatment would be beneficial (due to the intended enhancement of NK and T effector cells) or adverse (due to enhancement of the immunosuppressive activity of Treg) to cure. Complicating this debate is the question of whether the IL-2–induced FOXP3$^+$ T cells are bona fide Tregs. Data about their suppressive function are inconsistent (14–16) and transient expression of FOXP3 is also an established property of activated effector T cells (24). Our data now confirm that cells with multiple Treg characteristics including CD25 and FOXP3 expression and *FOXP3* TSDR demethylation are up-regulated after IL-2 therapy (Fig. 3*A*). Although still falling short of a functional test, these findings reiterate those concerns that IL-2 therapies stimulate natural Treg (16).

A converse treatment strategy is used for immunosuppression of transplantation patients. Transplantation patients receiving rATG showed a dramatic decrease of Treg (Fig. 3*B*), as would be expected from a therapy that unselectively depletes T cells. We also see a—less pronounced, but consistent for all tested patients—decrease of Treg following basiliximab therapy (Fig. 3*B*). The latter observation is unexpected because previous studies do not report a Treg decrease. Basiliximab's mode of action has been described as solely blocking the IL-2α receptor (CD25) without initiating cell depletion (43, 44). We cannot pinpoint the observed decrease of Treg on basiliximab exclusively because the therapy regimen includes other potent immunosuppressive factors, such as calcineurin inhibitors (tacrolimus), antiproliferate agents (mycophenolate mofetil), and corticosteroids (prednisone). At this point in time, we do not speculate on effects leading to or caused by the observed decrease of Treg during basiliximab treatment. Instead, our rationale behind the analyses performed was to exemplarily show that the qPCR assay is capable of monitoring the patients' Treg status. Taken together, we show that the effects of both, immunostimulatory and immunosuppressive therapy on Treg levels can be monitored using the presented qPCR assay.

We then investigated the idea that the *FOXP3* TSDR demethylation assay might provide a new, early indicator for the body's response to the existence of solid tumors, which can be analyzed in peripheral blood. We tested this hypothesis by conducting a blinded study that included patients with breast, prostate, colon, and lung tumors and compared those with healthy donors. In line with recent reports (39, 40), we showed that in blood from patients with lung and prostate cancers, significantly higher signals of Treg, i.e., demethylated *FOXP3* TSDR, were found compared with healthy controls. For patients with breast cancer, the Treg frequency determined by the demethylation assay was scarcely nonsignificant (P = 0.08) but still distinctly higher than in controls (Fig. 4). The results of *FOXP3* TSDR demethylation analysis in the peripheral blood of patients with colon cancer differ from previous results obtained by FACS, which showed an increase of FOXP3$^+$ cells compared with normal controls (45, 46). These differences might reflect the fact that the demethylation assay exclusively detects natural Treg. This is in contrast with the FACS analysis, which also detects other fractions of T cells transiently expressing FOXP3. Thus, if we speculate that all tumors take advantage of some suppressive immune function, it may be that the *FOXP3* TSDR demethylation assay falls short of identifying important other (transiently) FOXP3-expressing suppressive cells. Those cells may govern tumor immunity in colorectal cancer. Further research on both natural Treg and those other suppressive cell types is required. The search for epigenetic detection systems for these other cell types, including Tr1 cells, is ongoing in our laboratory.

Analysis of a larger number of patients and controls may clarify its significance to breast cancer and reconfirm those for lung and prostate cancer. Because it is assumed that markers which identify tumor patients with an AUC value of >0.7 are considered as potential diagnostic tools (47), *FOXP3* TSDR demethylation could

serve as an early detection marker for breast, lung, and prostate cancers. In our view, two major conclusions can be drawn from the results presented here: (*a*) this study encourages the idea to monitor Treg levels as variables for malignant tumor development in the body or the risk thereof; (*b*) further extensive studies are required for the various cancer entities and therapeutic approaches in order to validate *FOXP3* TSDR demethylation as a marker in the various settings.

We also investigated the applicability of the *FOXP3* TSDR demethylation assay as an alternative for the laborious and sometimes imprecise and biased immunohistochemistry analyses currently used for the measurement of Treg in fixed tissue samples (Fig. 5). Our analyses showed that the performance of both technologies is equivalent as far as distinction of cancer compared with healthy tissue is concerned. When taking into account that *FOXP3* TSDR demethylation is fully quantitative, performed without field/slide selection bias, is technically less demanding and independent of antibody performances, it seems to be the adequate tool for routine applications. Consequently, we believe that the low technical demands of the assay here will allow a significant acceleration of research and standardization of routine testing of tumor-infiltrating Treg. Biologically, our data obtained with both *FOXP3* TSDR demethylation and immunohistochemistry assays confirm an accumulation of Treg in lung and colon carcinoma tissue compared with their healthy adjacent tissues. This supports previous findings which suggest that an increased prevalence of Treg in the microenvironments of solid epithelial tumors (48) as reported for invasive breast, pancreas (6), hepatic (5), and lung (49) tumors. The implementation of a precise and routine testing of solid tissues for Treg becomes particularly important because there are various reports which suggest Treg as an important prognostic factor for disease outcome, as shown for ovarian cancer or breast cancer (11, 12).

In conclusion, we believe that the presented assay for quantitative Treg detection will, in the future, lead to better interstudy comparability, and faster and more efficient analysis even of FFPE tissues. Furthermore, our findings render the measurement of Treg frequency by analysis of the *FOXP3* TSDR methylation status a prime target not only for early tumor recognition but also for monitoring antitumor strategies.

Disclosure of Potential Conflicts of Interest

U. Baron, U. Hoffmüller, and S. Olek: Ownership interest, Epiontis. A. Hamann: Ownership interest, Charité. The other authors disclosed no potential conflicts of interest.

Acknowledgments

Received 6/20/2008; revised 9/10/2008; accepted 10/30/2008.

Grant support: Investitionsbank Berlin; the Wilhelm Sander Foundation and by the Deutsche Forschungsgemeinschaft (SFB633 and SFB650; J. Huehn).

The costs of publication of this article were defrayed in part by the payment of page charges. This article must therefore be hereby marked *advertisement* in accordance with 18 U.S.C. Section 1734 solely to indicate this fact.

We thank Alexander Hellwag for technical assistance, Michael Weber for advice, and Dirk Nargorsen for providing sample information. We owe Alex Olek for making our concept thinkable.

References

1. Sakaguchi S. Naturally arising $CD4^+$ regulatory T cells for immunologic self-tolerance and negative control of immune responses. Annu Rev Immunol 2004;22:531–62.
2. Valencia X, Lipsky PE. $CD4^+$ $CD25^+$ $FoxP3^+$ regulatory T cells in autoimmune diseases. Nat Clin Pract Rheumatol 2007;11:619–26.
3. Viglietta V, Baecher-Allan C, Weiner HL, Hafler DA. Loss of functional suppression by $CD4^+CD25^+$ regulatory T cells in patients with multiple sclerosis. J Exp Med 2004;199:971–9.
4. Huan J, Culbertson N, Spencer L, et al. Decreased FOXP3 levels in multiple sclerosis patients. J Neurosci Res 2005;81:45–52.
5. Ormandy LA, Hillemann T, Wedemeyer H, Manns MP, Greten TF, Korangy, F. Increased populations of regulatory T cells in peripheral blood of patients with hepatocellular carcinoma. Cancer Res 2005;65:2457–64.
6. Liyanage UK, Moore TT, Joo HG, et al. Prevalence of regulatory T cells is increased in peripheral blood and tumor microenvironment of patients with pancreas or breast adenocarcinoma. J Immunol 2002;169:2756–61.
7. Viguier M, Lemaître F, Verola O, et al. Foxp3 expressing $CD4^+CD25^{high}$ regulatory T cells are overrepresented in human metastatic melanoma lymph nodes and inhibit the function of infiltrating T cells. J Immunol 2004;173:1444–53.
8. Sasada T, Kimura M, Yoshida Y, Kanai M, Takabayashi A. $CD4^+CD25^+$ regulatory T cells in patients with gastrointestinal malignancies: possible involvement of regulatory T cells in disease progression. Cancer 2003;98: 1089–99.
9. Ichihara F, Kono K, Takahashi A, Kawaida H, Sugai H, Fujii H. Increased populations of regulatory T cells in peripheral blood and tumor-infiltrating lymphocytes in patients with gastric and esophageal cancers. Clin Cancer Res 2003;9:4404–8.
10. Beyer M, Schultze JL. Regulatory T cells in cancer. Blood 2006;108:804–11.
11. Curiel TJ, Coukos G, Zou L, et al. Specific recruitment of regulatory T cells in ovarian carcinoma fosters immune privilege and predicts reduced survival. Nat Med 2004;10:942–9.
12. Bates GJ, Fox SB, Han C, et al. Quantification of regulatory T cells enables the identification of high-risk breast cancer patients and those at risk of late relapse. J Clin Oncol 2006;24:5373–80.
13. Malek TR, Bayer AL. Tolerance, not immunity, crucially depends on IL-2. Nat Rev Immunol 2004;9: 665–74.
14. Cesana GC, DeRaffele G, Cohen S, et al. Characterization of $CD4^+CD25^+$ regulatory T cells in patients treated with high-dose interleukin-2 for metastatic melanoma or renal cell carcinoma. J Clin Oncol 2006;24:1169–77.
15. van der Vliet HJ, Koon HB, Yue SC, et al. Effects of the administration of high-dose interleukin-2 on immunoregulatory cell subsets in patients with advanced melanoma and renal cell cancer. Clin Cancer Res 2007; 13:2100–8.
16. Ahmadzadeh M, Rosenberg SA. IL-2 administration increases $CD4^+$ $CD25^{(hi)}$ $Foxp3^+$ regulatory T cells in cancer patients. Blood 2006;107:2409–14.
17. Bonnefoy-Bérard N, Vincent C, Revillard JP. Antibodies against functional leukocyte surface molecules in polyclonal antilymphocyte and antithymocyte globulins. Transplantation 1991;51:669–73.
18. Nashan B, Moore R, Amlot P, Schmidt AG, Abeywickrama K, Soulillou JP; CHIB 201 International Study Group. Randomised trial of basiliximab versus placebo for control of acute cellular rejection in renal allograft recipients. Lancet 1997;350:1193–8.
19. Bennett CL, Christie J, Ramsdell F, et al. The immune dysregulation, polyendocrinopathy, enteropathy, X-linked syndrome (IPEX) is caused by mutations of FOXP3. Nat Genet 2001;27:20–1.
20. Fontenot JD, Gavin MA, Rudensky AY. Foxp3 programs the development and function of $CD4^+$ $CD25^+$ regulatory T cells. Nat Immunol 2003;4:330–6.
21. Hori S, Nomura T, Sakaguchi S. Control of regulatory T cell development by the transcription factor Foxp3. Science 2003;299:1057–61.
22. Fontenot JD, Rasmussen JP, Williams LM, Dooley JL, Farr AG, Rudensky AY. Regulatory T cell lineage specification by the forkhead transcription factor foxp3. Immunity 2005;22:329–41.
23. Wan YY, Flavell RA. Identifying Foxp3-expressing suppressor T cells with a bicistronic reporter. Proc Natl Acad Sci U S A 2005;102:5126–31.
24. Ziegler SF. FOXP3: not just for regulatory T cells anymore. Eur J Immunol 2007;37:21–3.
25. Walker MR, Kasprowicz DJ, Gersuk VH, et al. Induction of FoxP3 and acquisition of T regulatory activity by stimulated human $CD4^+CD25^-$ T cells. J Clin Invest 2003;112:1437–43.
26. Roncador G, Brown PJ, Maestre L, et al. Analysis of FOXP3 protein expression in human $CD4^+CD25^+$ regulatory T cells at the single-cell level. Eur J Immunol 2005;35:1681–91.
27. Loddenkemper C, Schernus M, Noutsias M, Stein H, Thiel E, Nagorsen D. *In situ* analysis of $FOXP3^+$ regulatory T cells in human colorectal cancer. J Transl Med 2006;4:52.
28. Floess S, Freyer J, Siewert C, et al. Epigenetic control of the foxp3 locus in regulatory T cells. PLoS Biol 2007; 5:e38.
29. Baron U, Floess S, Wieczorek G, et al. DNA demethylation in the human FOXP3 locus discriminates regulatory T cells from activated $FOXP3(^+)$ conventional T cells. Eur J Immunol 2007;37:2378–89.
30. Bird A. DNA methylation patterns and epigenetic memory. Genes Dev 2002;16:6–21.
31. Baron U, Türbachova I, Hellwag A, et al. DNA methylation analysis as a tool for cell typing. Epigenetics 2006;1:55–60.
32. Eckhardt F, Lewin J, Cortese R, et al. DNA methylation profiling of human chromosomes 6, 20 and 22. Nat Genet 2006;38:1378–85.
33. Huehn J, Siegmund K, Lehmann JC, et al. Developmental stage, phenotype, and migration distinguish naive- and effector/memory-like $CD4^+$ regulatory T cells. J Exp Med 2004;199:303–13.
34. Asemissen AM, Scheibenbogen C, Letsch A, et al. Addition of histamine to interleukin 2 treatment augments type 1 T-cell responses in patients with melanoma *in vivo*: immunologic results from a

randomized clinical trial of interleukin 2 with or without histamine (MP 104). Clin Cancer Res 2005;11: 290–7.
35. Loddenkemper C, Maul J, Berg E, Stein H, Zeitz M, Duchmann R. Analysis of FOXP3 protein expression in human $CD4^+$ $CD25^+$ regulatory T cells at the single-cell level. Eur J Immunol 2006;36:245.
36. Olek A, Oswald J, Walter J. A modified and improved method for bisulphite based cytosine methylation analysis. Nucleic Acids Res 1996;24:5064–6.
37. Rasmussen R. Quantification on the LightCycler. In: Meuer S, Wittwer C, Nakagawara K, editors. Rapid cycle real-time PCR, methods and applications. Heidelberg: Springer Press; 2001. p. 21–34.
38. DeLong ER, DeLong DM, Clarke-Pearson DL. Comparing the areas under two or more correlated receiver operating characteristic curves: a nonparametric approach. Biometrics 1988;44:837–45.
39. Meloni F, Morosini M, Solari N, et al. Foxp3 expressing $CD4^+CD25^+$ and $CD8^+CD28^-$ T regulatory cells in the peripheral blood of patients with lung cancer and pleural mesothelioma. Hum Immunol 2006;67:1–12.
40. Miller AM, Lundberg K, Ozenci V, et al. $CD4^+CD25^{high}$ T cells are enriched in the tumor and peripheral blood of prostate cancer patients. J Immunol 2006;177:7398–405.
41. Zuo T, Wang L, Morrison C, et al. FOXP3 is an X-linked breast cancer suppressor gene and an important repressor of the HER-2/ErbB2 oncogene. Cell 2007;129:1275–86.
42. Zenclussen AC. $CD4^+$ $CD25^+$ T regulatory cells in murine pregnancy. J Reprod Immunol 2005;65:101–10.
43. Game DS, Hernandez-Fuentes MP, Lechler RI. Everolimus and basiliximab permit suppression by human $CD4^+$ $CD25^+$ cells *in vitro*. Am J Transplant 2005;5:454–64.
44. Tkaczuk J, Yu CL, Baksh S, et al. Effect of anti-IL-2R α antibody on IL-2-induced Jak/STAT signaling. Am J Transplant 2002;2:31–40.
45. Clarke SL, Betts GJ, Plant A, et al. $CD4^+$ $CD25^+$ $FOXP3^+$ regulatory T cells suppress anti-tumor immune responses in patients with colorectal cancer. PLoS ONE 2006;1:e129.
46. Ling KL, Pratap SE, Bates GJ, et al. Increased frequency of regulatory T cells in peripheral blood and tumour infiltrating lymphocytes in colorectal cancer patients. Cancer Immun 2007;7:7.
47. Lofton-Day C, Model F, Devos T, et al. DNA methylation biomarkers for blood-based colorectal cancer screening. Clin Chem 2008;54:414–23.
48. Woo EY, Chu CS, Goletz TJ, et al. Regulatory $CD4^+$ $CD25^+$ T cells in tumors from patients with early-stage non-small cell lung cancer and late-stage ovarian cancer. Cancer Res 2001;61:4766–72.
49. Petersen RP, Campa MJ, Sperlazza J, et al. Tumor infiltrating $Foxp3^+$ regulatory T-cells are associated with recurrence in pathologic stage I NSCLC patients. Cancer 2006;10:2866–72.